



TITLE:

On the Strain Distribution and Failure of Wood Plates with a Round Knot under Tensile Load

AUTHOR(S):

SASAKI, Hikaru; MAKU, Takamaro

CITATION:

SASAKI, Hikaru ...[et al]. On the Strain Distribution and Failure of Wood Plates with a Round Knot under Tensile Load. 木材研究: 京都大学木材研究所報告 1962, 28: 1-23

ISSUE DATE:

1962-08

URL:

<http://hdl.handle.net/2433/52901>

RIGHT:

On the Strain Distribution and Failure of Wood Plates with a Round Knot under Tensile Load

Wood Physics, Section 2 Hikaru SASAKI and Takamaro MAKU

佐々木光・満久崇磨：引張を受ける有節板のひずみ分布と破壊について

Introduction

Almost all timbers include the knot which is one of the most common defects and reduces considerably the strength of timber and, therefore, the research on the mechanical properties of knotty wood is very important. But, in general, there are various types of knots and the grain of its surroundings differs so much that one cannot, without any difficulties, classify the mechanical properties of knotty wood and find any rules which will exist there. Thus, there are very few reports about them especially under tensile load, for example, on the tensile strength: O. GRAF (1929)¹⁾, E. GABER (1935)²⁾ and T. MORI (1938)³⁾, and on the tensile strain distribution: A. YLINEN (1942)⁴⁾. This is the reason why the timber have mostly been used as compression or bending members but not as a tension member in wood constructions. But, recently, with the advance of the architectural-style, -technique, -materials etc., timber is being used as a tension member of constructions, for example, as the flange of a box-beam.

In the present paper, we investigated some mechanical properties of wood plates with a round knot under tensile load. The paper can be generously divided into following two parts.

1. The strain distribution of knotty plate by means of the brittle coating method, about which we hitherto carried out many fundamental experiments for applying it to wood⁵⁾ and by which we solved experimentally some two-dimensional problems of wood⁶⁾.

2. Where the fracture of a specimen takes place and grows, and at what kind of stress the specimen breaks.

The knotty plates in this paper were cut out of a wood stock having one knot, and had a group of the round knots which varies continuously from sound knot to loose knot (ref. Fig. 1).

Here, "Fracture", "Rupture" and "Failure" mean in the present paper as follows:

Fracture — a local failure of a specimen which takes place while the load is increasing.

Rupture — a state where a specimen breaks in two separated parts.

Failure — general expression which contains “Fracture” and “Rupture”.

Materials and Methods

1. Materials and specimens

A knotty wood stock of HINOKI (*Chamaecyparis obtusa* ENDL.) shown in Fig. 1-a was used, and its upper side (outer-most face of xylem) is shown in Photo. 1. The stock was sawn into nineteen plates (3 mm thick) with a round knot in their central part respectively, and they were numbered from bark side to pith (Fig. 1-a).

The outer-most plate (No. 0) and the inner-most one (No. 18) were omitted from the test because of their ununiformity in thickness.

The plates were piled up and air-dried carefully for three months in a room in order to avoid their warping, and then

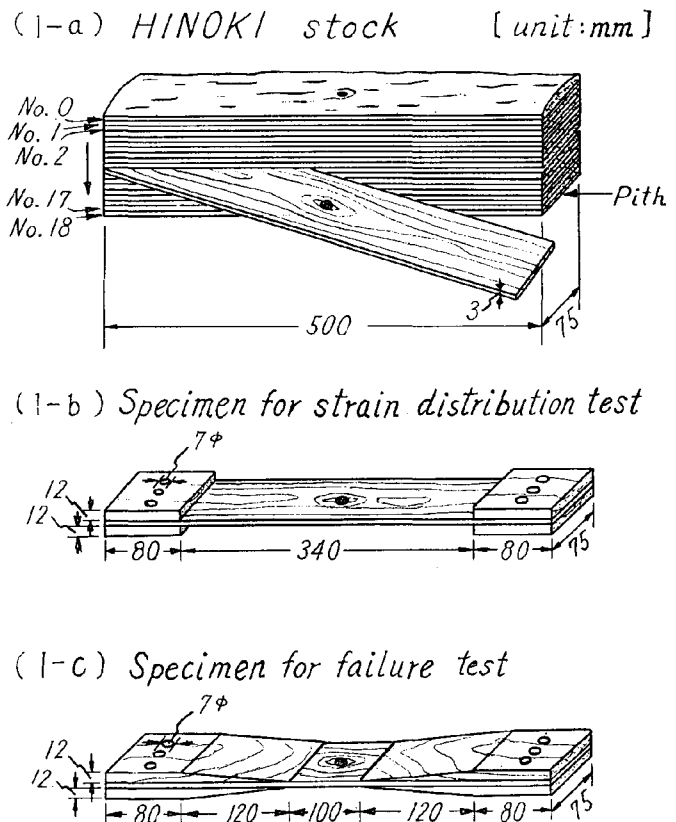


Fig. 1. Specimens and HINOKI stock of which knotty thin plates were cut out.

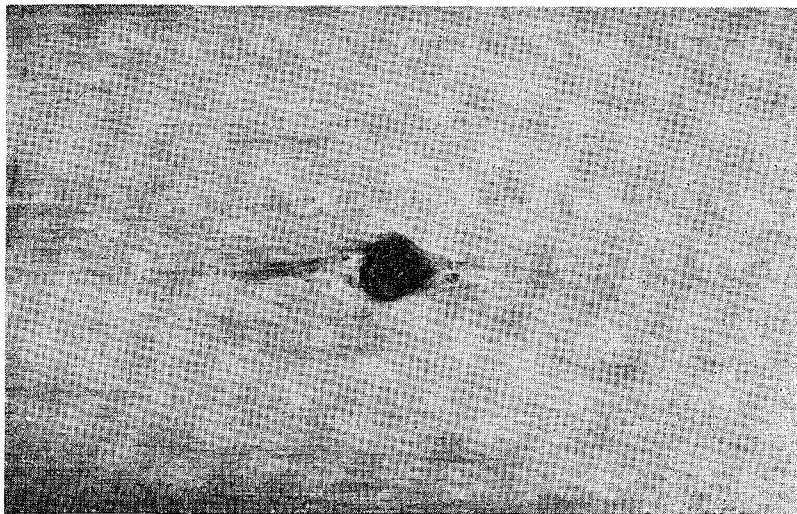


Photo. 1. External appearance of xylem of HINOKI stock used in this experiment.

finished by files and sanding papers. Then, the plates of even numbers were used to the determination of the strain distribution, and those of odd numbers to the failure tests.

The test specimens are as shown in Fig. 1-b (strain determination) and in Fig. 1-c (failure test). As shown in these figures, the grips of specimens were reinforced by HINOKI blocks which were bonded to the specimen with urea formaldehyde resin, and three holes of 7 mm diameter were bored in each of them in order to clamp them to the head of the testing machine. Table 1 shows the dimensions and the details of the specimens.

Table 1. Dimensions and details of specimens.

Specimen No.	Distance from pith to each specimen	Type of test*	Width of specimen b	Thickness of specimen h	Diameter of knot ϕ
1	77 mm	C	7.28 ^{cm}	0.25 ^{cm}	1.01 ^{cm}
2	72.5	B	7.78	0.31	1.10
3	68	C	7.35	0.27	1.10
4	63.5	B	7.87	0.32	1.30
5	59	C	7.29	0.25	1.30
6	54.5	B	7.86	0.26	1.40
7	50	C	7.13	0.27	1.39
8	45.5	B	7.86	0.27	1.40
9	41	C	7.17	0.26	1.31
10	36.5	B	7.79	0.30	(1.3)**
11	32	C	7.05	0.28	(1.3)
12	27.5	B	7.70	0.24	(1.2)
13	23	C	7.28	0.29	(1.2)
14	18.5	B	7.73	0.30	(0.8)
15	14	C	7.19	0.27	(0.7)
16	9.5	B	7.68	0.28	(0.3)
17	5	C	7.23	0.25	(0.2)

* C : Failure test (specimen-Fig. 1-c).

B : Strain distribution test (Fig. 1-b).

** () : Diameter of sound knot.

As the knot of the stock was almost perpendicular to the pith, the knot of each specimen was nearly round. But, it is rather difficult, actually, to determine the diameter of a sound knot, and herein, for the sake of convenience, we defined it as that of the largest but round annual ring in a sound knot. And the values shown in Table 1 are that perpendicular to the load direction.

2. Test methods

a) Determination of strain distribution

Determination of strain distribution of the knotty plates was carried out by the brittle coating method. The procedure of which is summarized as follows :

After the specimens were sealed with black enamel (under-coating), a kind of strain sensitive lacquer known on the market in Japan was sprayed on face and back of these specimens in uniform thickness of 0.1 mm.

It must be noticed that before the lacquer is sprayed, a loose (holed) knot should be completely set with rubber in order to avoid the irregularity of the coating thickness along the border of the knot.

The composition of the lacquer is a phenol resin and titan white dissolved in mixture of benzen, toluene and xylene.

When the coating was dried at $5\sim 10^{\circ}\text{C}$ for about twenty days and the "strain sensitivity" reached about 0.25%, the load which is about 50~80% of the tensile strength of knotty wood was applied to the specimen. And the crack pattern produced

was stained with pararosaniline solution.

Crack densities at each point of specimens were converted into strain by the relation between crack density and strain which was obtained from cantilever calibrating strips simultaneously tested under the same conditions.

b) Observation of fracture and rupture

Specimens were loaded by lever-type 2-ton universal testing machine, the attachment of which is as shown in Fig. 2 (the same method was also applied to the strain distribution test). The rate of loading was $100\text{ kg/cm}^2\cdot\text{min}$. The fracture and its growth were marked under loading and finally the maximum load at the

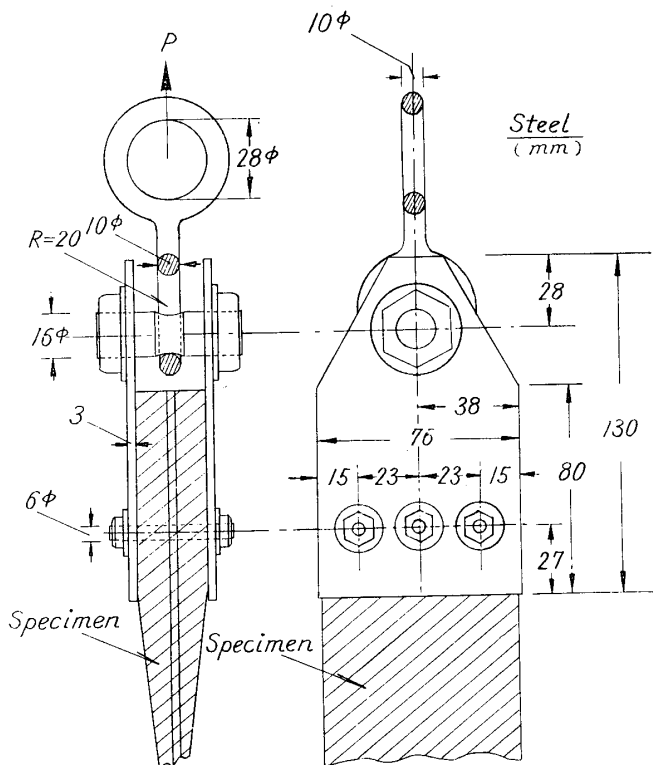


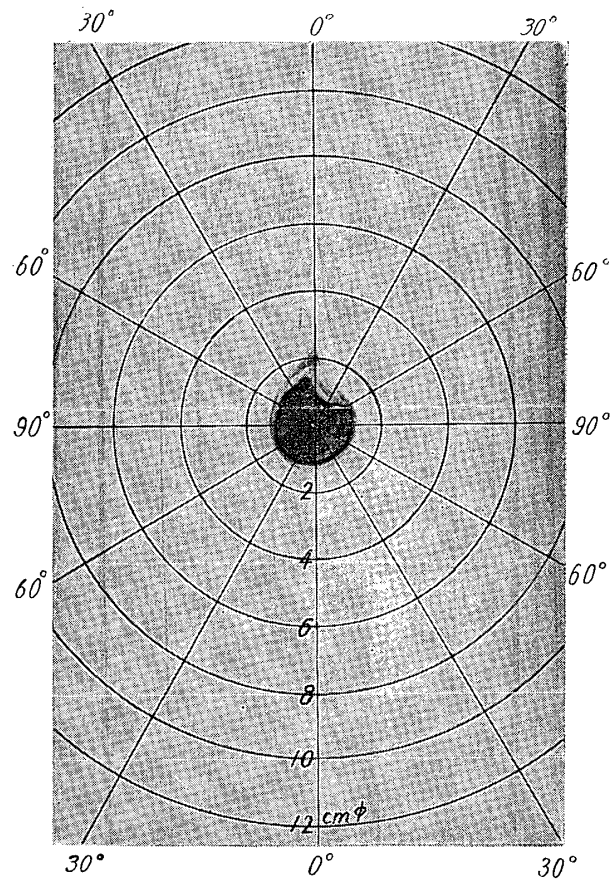
Fig. 2. Attachment for clamping specimen to the head of the tensile testing machine.

rupture was obtained.

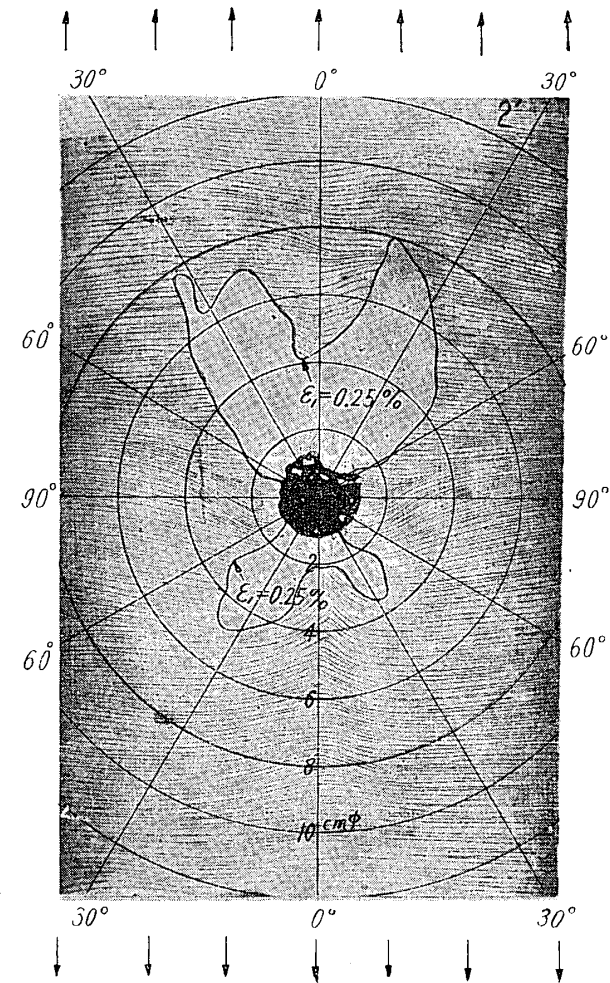
Results and Discussion

1. Strain distribution

Crack patterns gotten on the pith side face of each specimen of No. 2, 4, 6, 8, 10 and 12, are shown in Photos. 2, 3, 4, 5, 6 and 7 respectively, in comparison with their grain figures. In No. 14 and 16 specimens, the failure took place, however, in



(a)



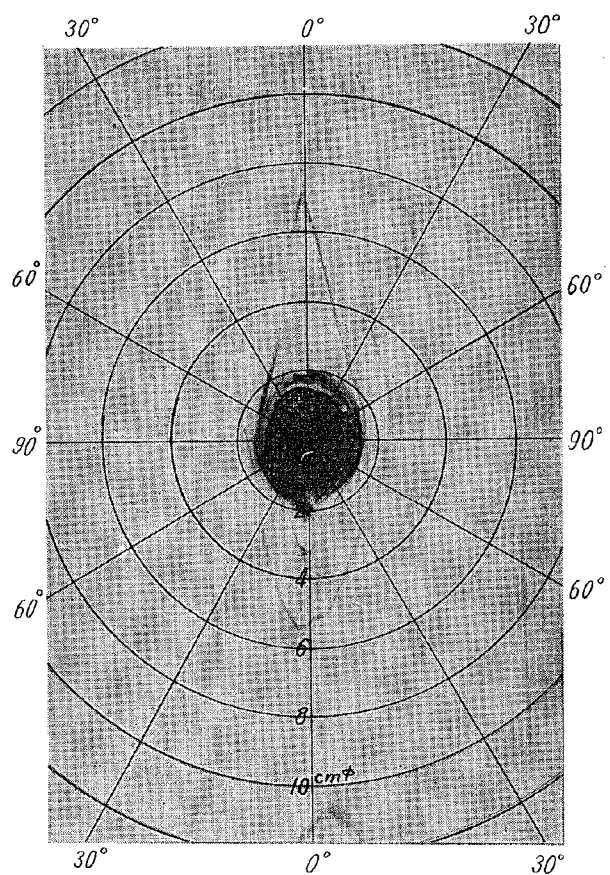
(b)

Photo. 2. Crack pattern of coating on a knotty plate (Specimen No. 2) by tension in comparison with the grain figure.

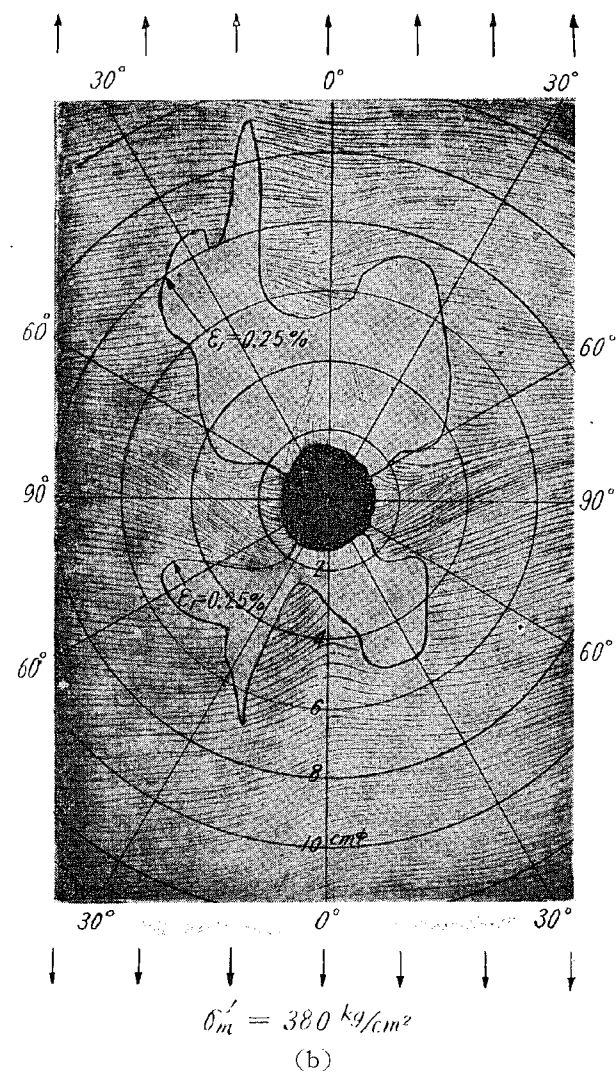
(a) Grain figure of specimen.

(b) Crack pattern of coating.

$$\sigma_m = 470 \text{ kg/cm}^2$$



(a)

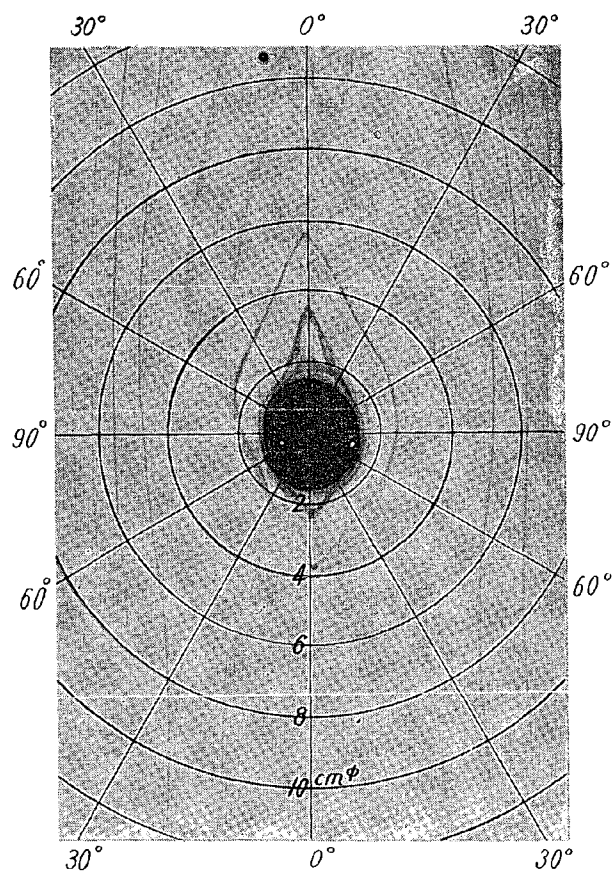


(b)

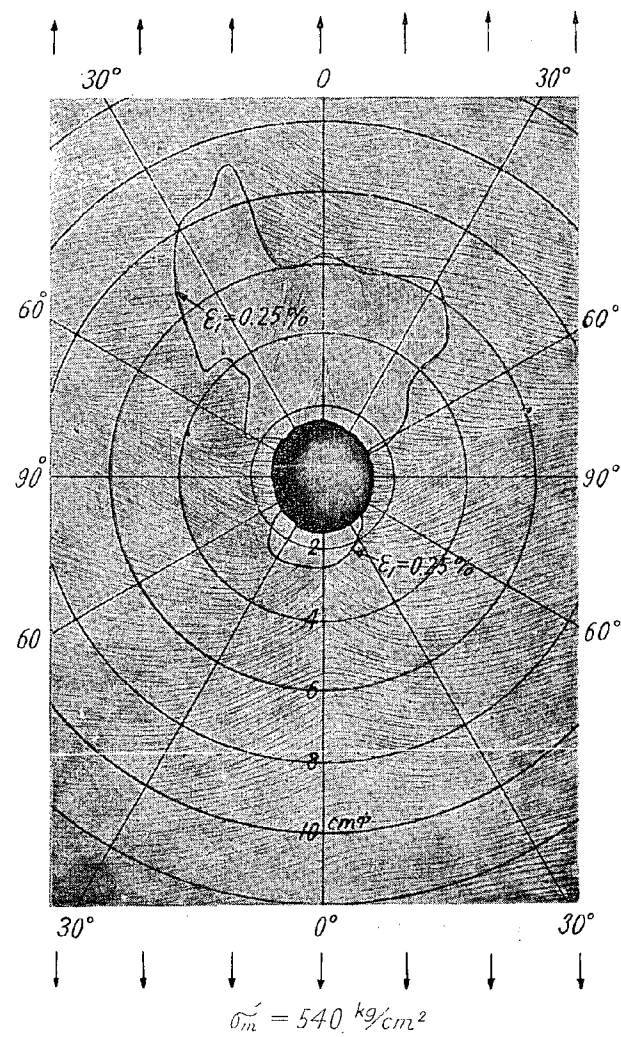
Photo. 3. Crack pattern of coating on a knotty plate (Specimen No. 4) by tension in comparison with the grain figure.

(a) Grain figure of specimen.

(b) Crack pattern of coating.



(a)

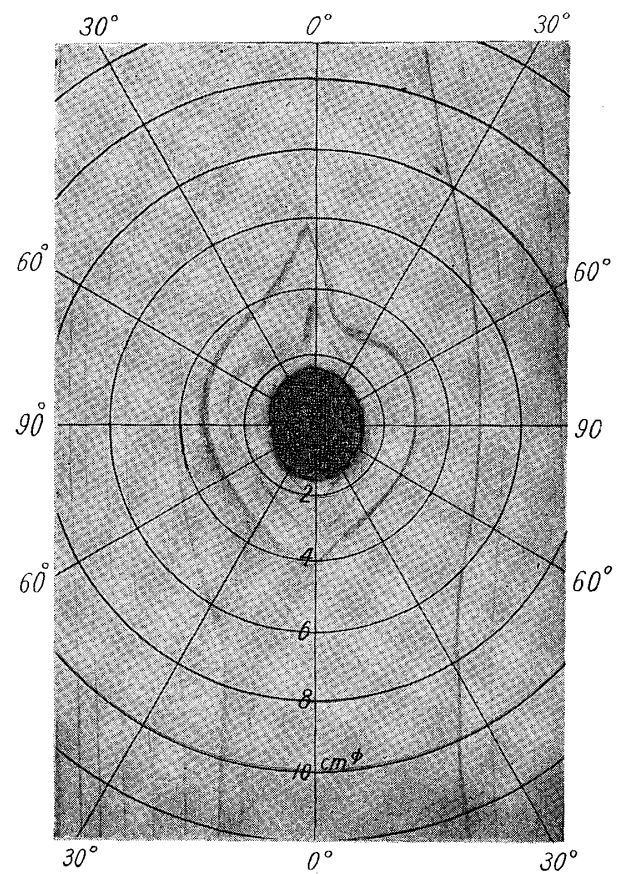


(b)

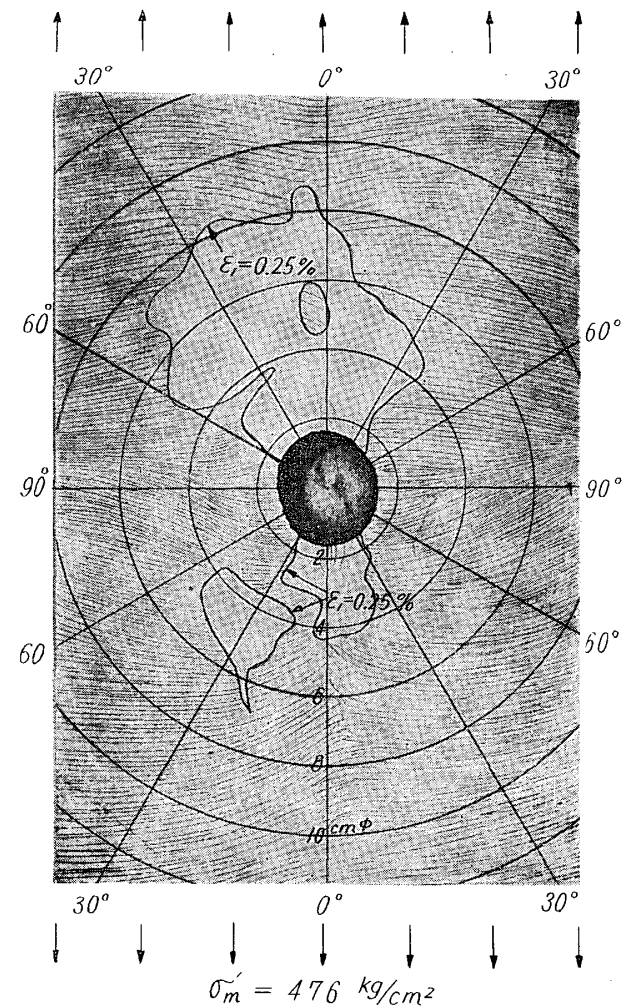
Photo. 4. Crack pattern of coating on a knotty plate (Specimen No. 6) by tension in comparison with the grain figure.

(a) Grain figure of specimen.

(b) Crack pattern of coating.



(a)

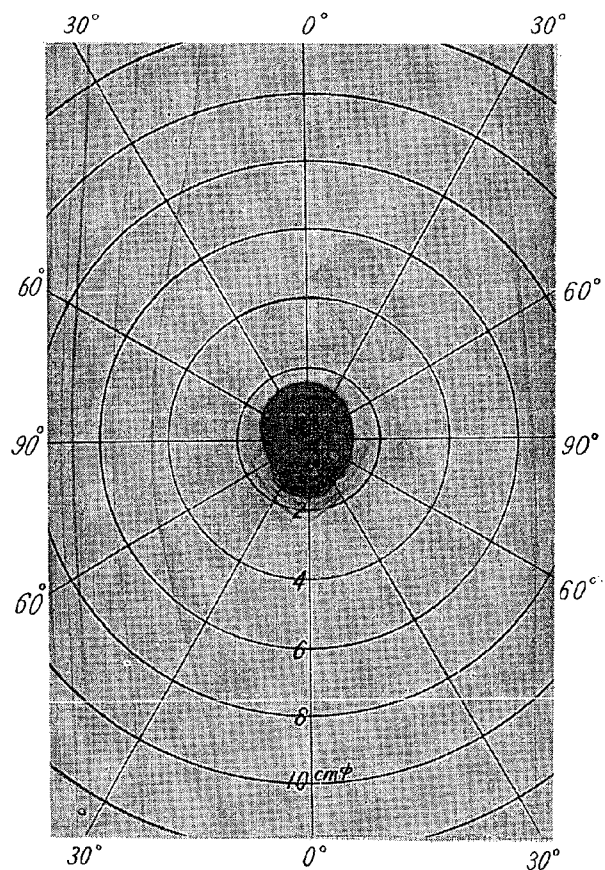


(b)

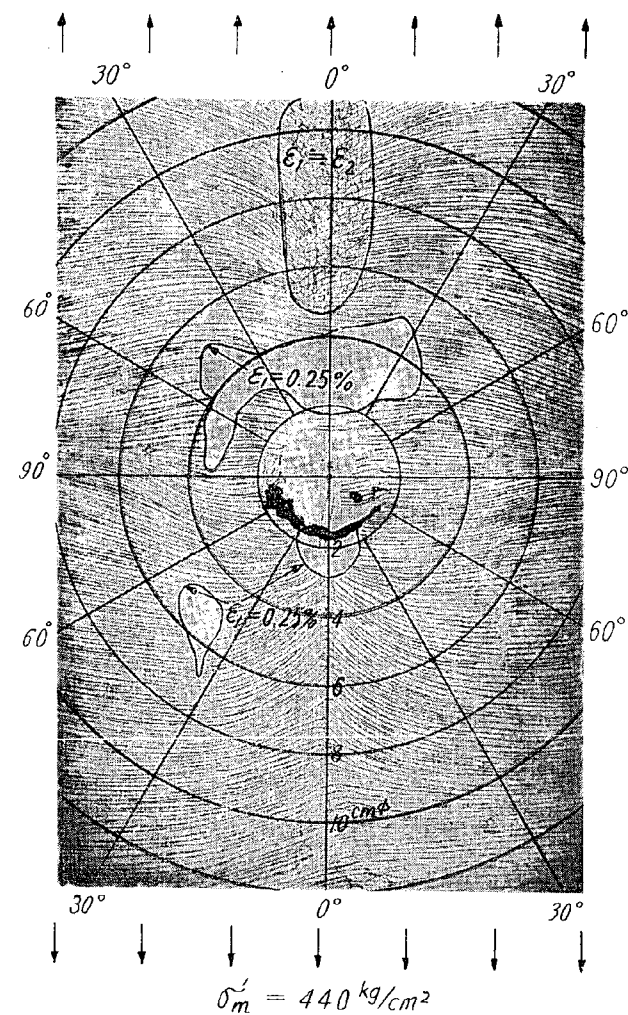
Photo. 5. Crack pattern of coating on a knotty plate (Specimen No. 8) by tension in comparison with the grain figure.

(a) Grain figure of specimen.

(b) Crack pattern of coating.



(a)

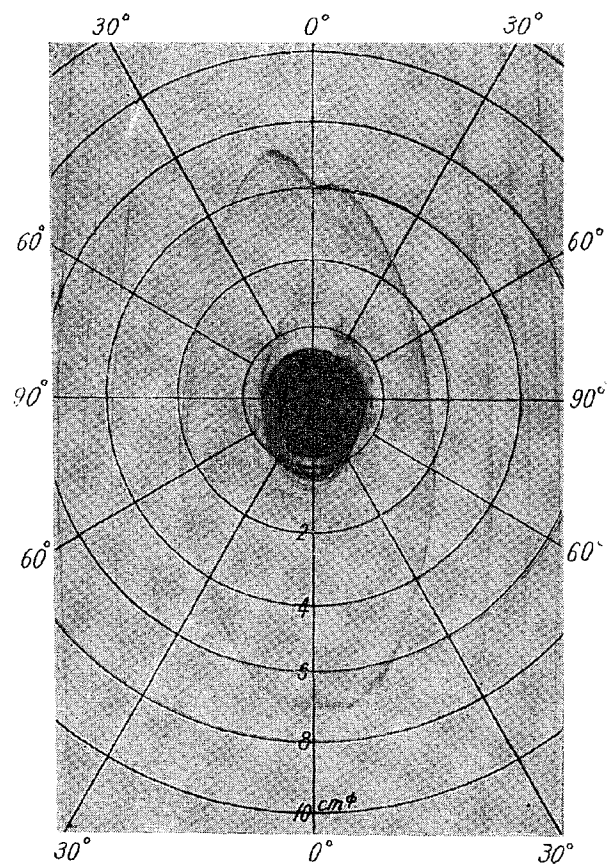


(b)

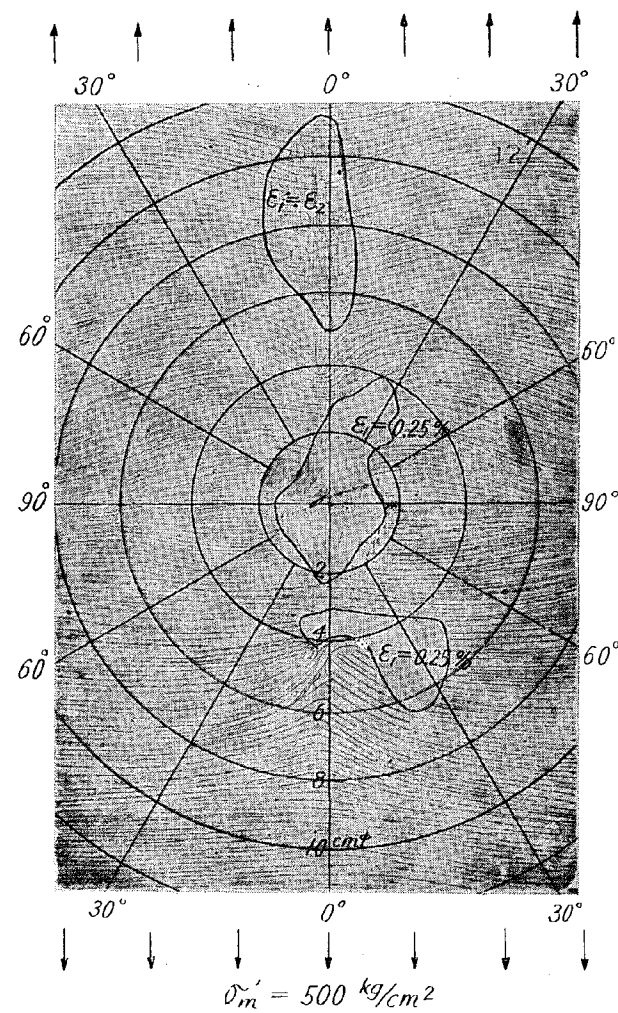
Photo. 6. Crack pattern of coating on a knotty plate (Specimen No. 10) by tension in comparison with the grain figure.

(a) Grain figure of specimen.

(b) Crack pattern of coating.



(a)



(b)

Photo. 7. Crack pattern of coating on a knotty plate (Specimen No. 12) by tension in comparison with the grain figure.

(a) Grain figure of specimen.

(b) Crack pattern of coating.

the vicinity of grips, so the crack patterns could not be gotten.

There exists considerable differences between a crack pattern of a knotty plate and that of a holed (artificially) wood plate (Photo. 8)⁶⁾. These characteristics of crack patterns on the knotty specimens are summarized as follows :

i) Shapes of loci on which the maximum tensile strain is equivalent (that is called "isoevantic line") are very irregular in comparison with those of simply holed plates. Above all, those of the plates with a loose knot (Photos. 2~5) spread widely and very irregularly over the upper portion of the knot in photographs (also in the trunks). They, generally, seem to have some connections with the grain figures.

ii) In the plates with a sound knot, there appears the zones where two principal strains are almost equivalent ($\epsilon_1 \doteq \epsilon_2$) as shown in Photos. 6 and 7, and this seems to be caused by disarrangements of grain in the vicinity of a sound knot, which is widened just beside the knot and then narrowed. These zones must be, therefore, stretched laterally when tensile load is applied to the specimen, because the sound knot will not be able to reduce its dimension.

iii) Directions of principal strains (ϵ_1) around a loose knot are irregular very much. And strain distribution on the plate with a sound knot, is comparatively symmetrical about two axes of the rectangular co-ordinates, but the symmetry about the abscissa can not be found on the plate with a loose knot.

The conversion of crack densities into principal strains was tried on five lateral lines of 3 cm interval (ref. Fig. 3). The results are shown in Figs. 3~8, in which length and direction of rods show value and direction of ϵ_1 at that point respectively. These results are summarized as follows :

i) The highest value of ϵ_1 is produced not only just beside the knot but also at an edge of the specimen.

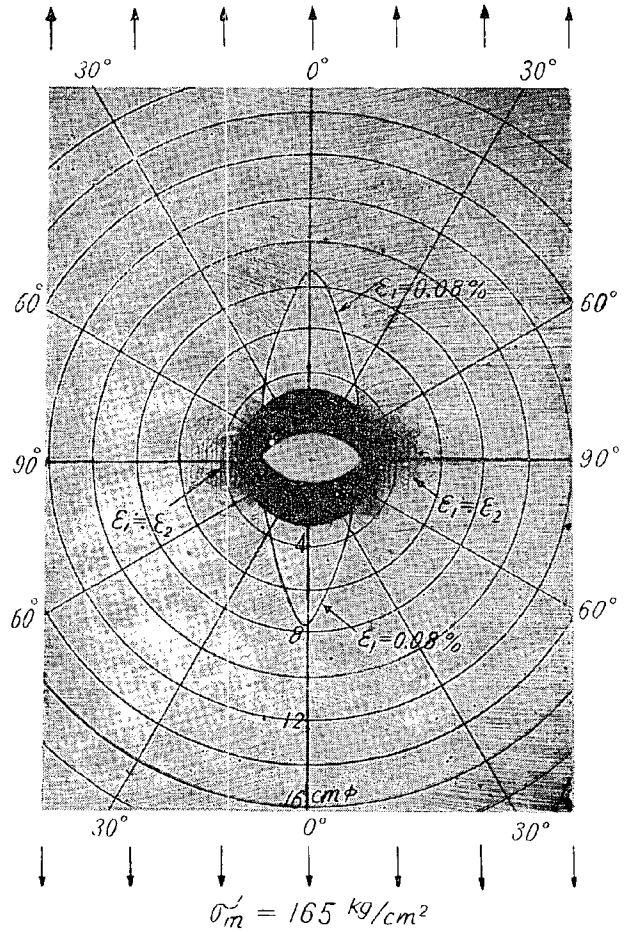


Photo. 8. Crack pattern of coating on a artificially holed plate by tension⁶⁾.

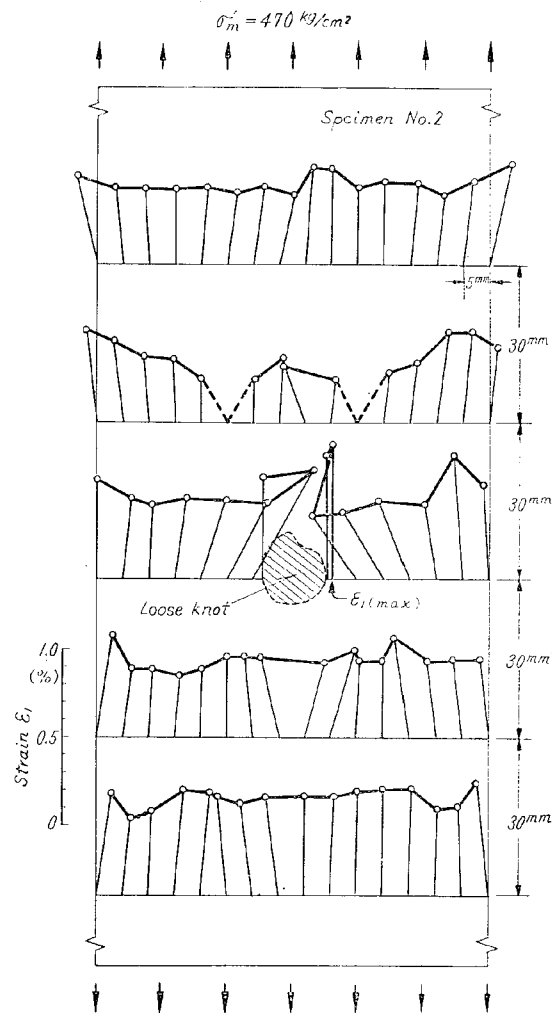


Fig. 3. Distribution of maximum principal strain in knotty plate under tensile load (Specimen No. 2).

Rods are drawn perpendicularly to maximum principal strain direction.

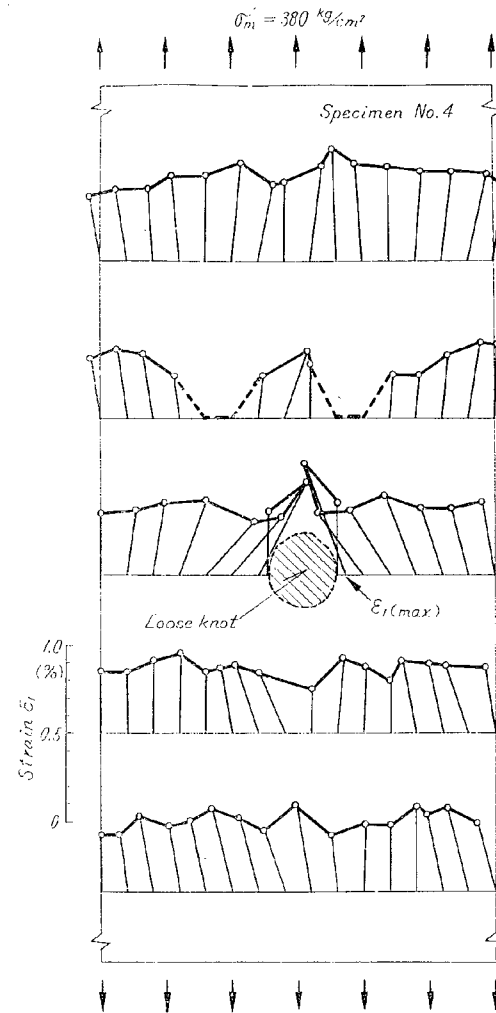


Fig. 4. Distribution of maximum principal strain in knotty plate under tensile load (Specimen No. 4).

Rods are drawn perpendicularly to maximum principal strain direction.

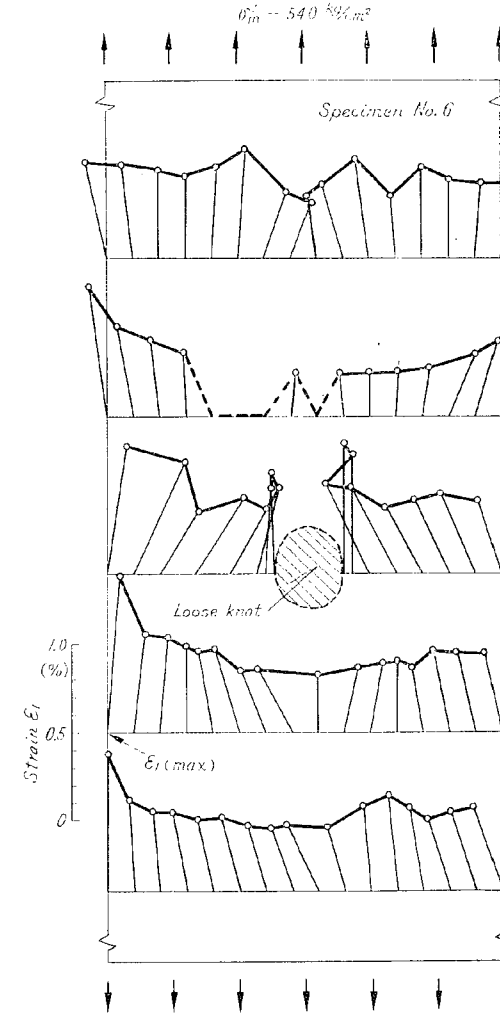


Fig. 5. Distribution of maximum principal strain in knotty plate under tensile load (Specimen No. 6).

Rods are drawn perpendicularly to maximum principal strain direction.

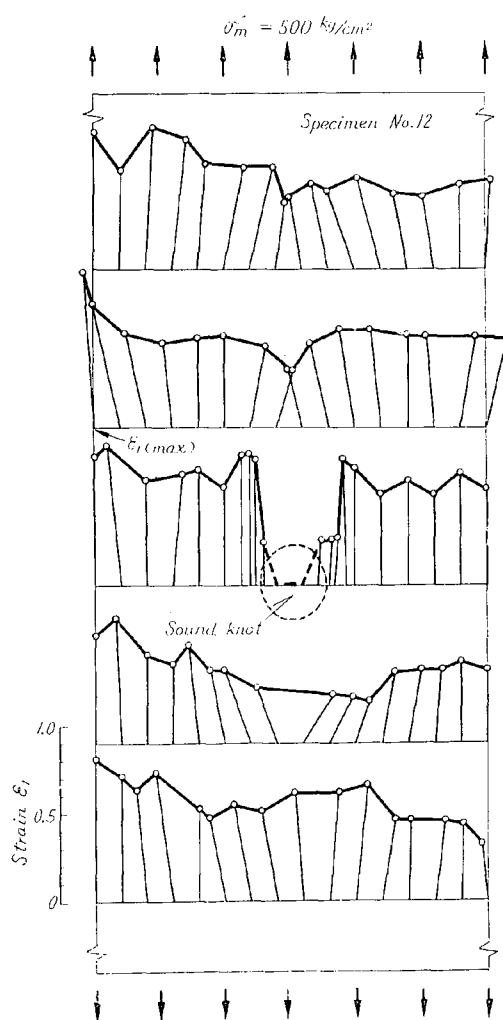


Fig. 6. Distribution of maximum principal strain in knotty plate under tensile load (Specimen No. 8).

Rods are drawn perpendicularly to maximum principal strain direction.

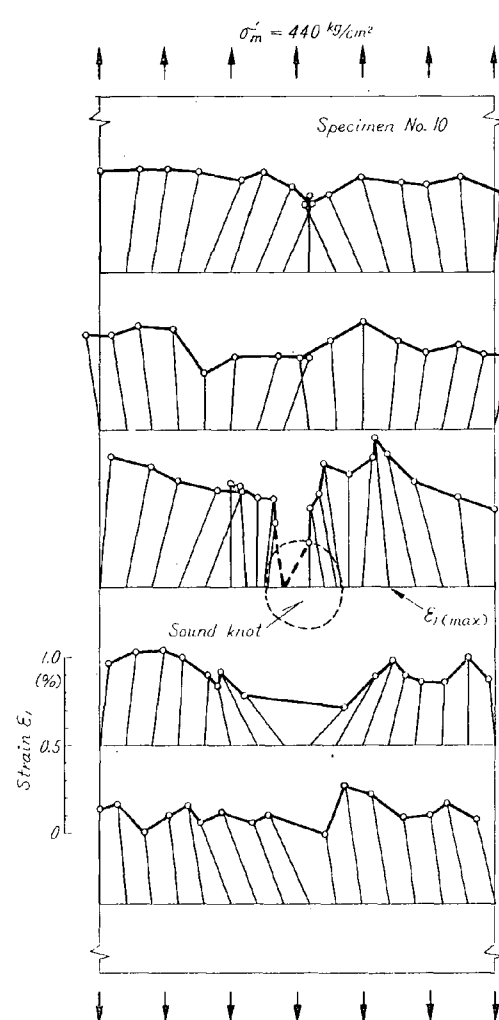


Fig. 7. Distribution of maximum principal strain in knotty plate under tensile load (Specimen No. 10).

Rods are drawn perpendicularly to maximum principal strain direction.

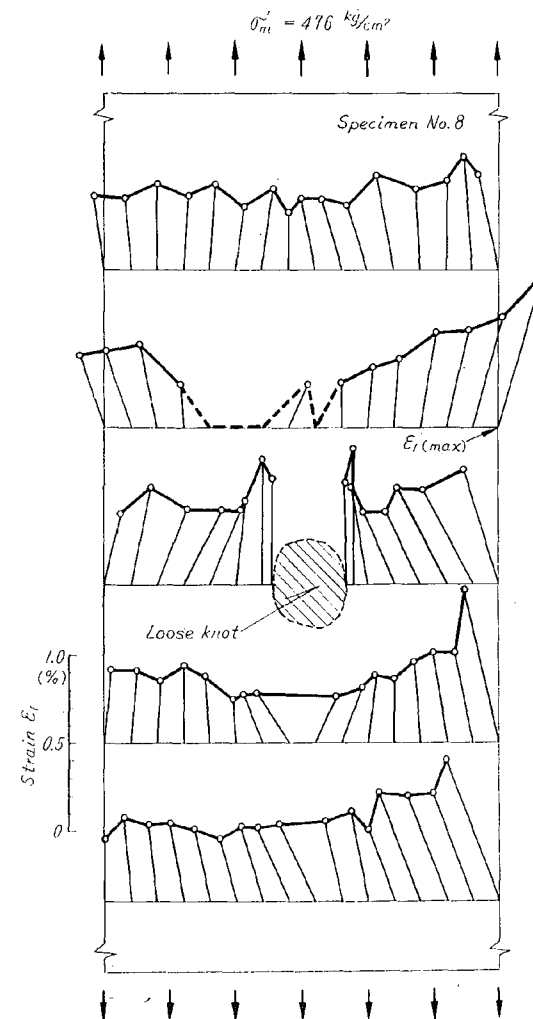


Fig. 8. Distribution of maximum principal strain in knotty plate under tensile load (Specimen No. 12).

Rods are drawn perpendicularly to maximum principal strain direction.

ii) In case of a loose knot, ϵ_1 on the lateral line acrossing the knot increases in the vicinity of the knot, but it does not always take the highest value at the border of the knot. Moreover, even the highest value of ϵ_1 is not higher than double of the average value of ϵ_1 of a cross section remoting from the knot, and this value is considerably lower than that of a simply holed plate in which the highest value of ϵ_1 is generally six times of the average value. So, it will be concluded that the border of a loose knot has high elastic modulus.

iii) On the other hand, large strains are not always appeared in the vicinity of a sound knot. And the deformation of a sound knot itself can not be clarified here, because the knot itself had broken before the crack pattern was stained.

Now, let us discuss the failure of these knotty specimens. First, because the

Table 2. Mechanical properties of knot-free portion of HINOKI used in this paper.

Tensile strength in fiber direction σ_0	$1250 \pm 142 \text{ kg/cm}^2$
Elastic modulus in fiber direction E	$8.9 \pm 1.91 \times 10^4 \text{ kg/cm}^2$
Shearing strength along fiber in radial plane τ_{RL}	$80 \pm 9.2 \text{ kg/cm}^2$
Modulus of rigidity along fiber in radial plane G_{RL}	$0.55 \pm 0.09 \times 10^4 \text{ kg/cm}^2$

elastic moduli will vary very much in the vicinity of a knot, we can not define the stress distribution from the strain distribution. But, if we can take "the maximum strain theory" on the failure of knotty wood, the tensile rupture will take place not only in the vicinity of knot but also at the edge of the specimen, and the latter may be related to the width of the specimen.

On the other hand, we can observe the difference between the direction of ϵ_1 and that of fiber, and there must be acting some shearing force along the fiber. Failure may take place there because the shear

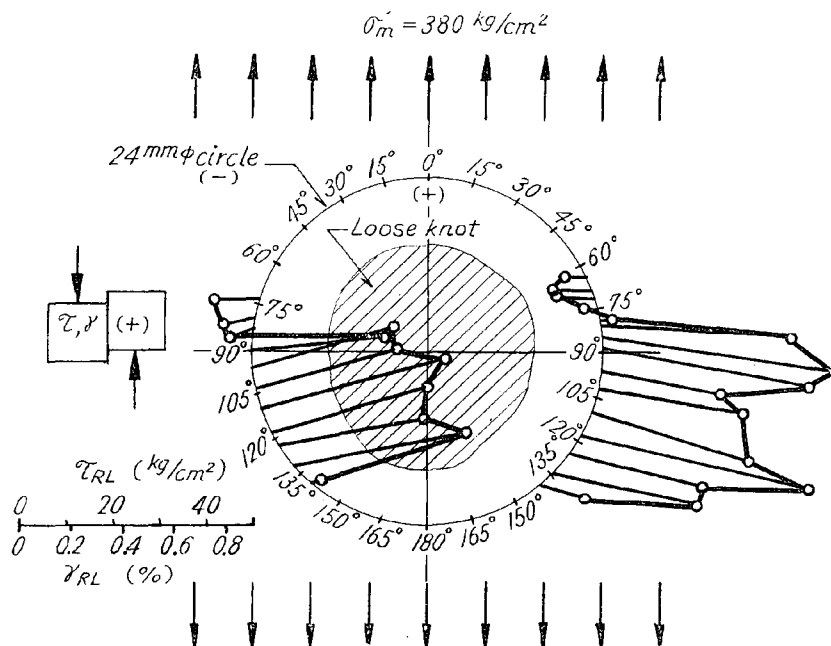


Fig. 9. Distribution of shear stress (strain) along fiber $\tau_{RL}(\gamma_{RL})$ on a circumference of 24 mm diameter around a knot (Specimen No. 4).

Rods are drawn perpendicularly to fiber.

strength along fiber of wood is not higher than $1/10 \sim 1/17^n$ of tensile strength parallel to the fiber. The strength and elastic constant in the knot-free portion of HINOKI in this experiment are measured and shown in Table 2.

In Fig. 9, for example, distribution of shear strain on the circumference (diameter : 24 mm) which was drawn around the knot in specimen No. 4 are shown. In this figure, $\varepsilon_2 = 0$ was assumed and the distribution of the shear stress was calculated under an assumption that the rigidity modulus is uniform and equal to that of knot-free portions ($G_{RL} \doteq 0.5 \times 10^4 \text{ kg/cm}^2$),

In the right half of the circumference, there distribute large shear strain or stress (< 0) in the range from 80° to 140° , and their maximum value is 0.91% or 50 kg/cm^2 . This value must be appreciated more highly because ε_2 will be, in this point, smaller than zero, so the fracture by this shear strain (or stress) will take place before the tensile rupture of specimen will do. This fracture will, however, not develop upwards through the point of 80° , because there is an inversion of the sign of shear strain (or stress) at this point. In the left half of the circumference, the distribution of shear strain (or stress) is roughly similar to that in the right one, but the sign is opposite.

2. Fracture and Rupture

Tensile stress of a plate with a round knot, can be shown by an average stress of the specimen as

$$\sigma_m = P/bh \dots \dots \dots (a)$$

(P : load, b : width of specimen, h : thickness of specimen),

or, by an average stress calculated by the reduced cross section of the specimen as

$$\sigma_k = P/(b-\phi)h \dots \dots \dots (b)$$

(ϕ : diameter of knot).

If the average tensile strength of knot-free specimen σ_0 is known, we may define the following factors by conversing the noting of "notch factor",

$$\left. \begin{array}{l} \beta_m = \sigma_0/\sigma_m \\ \beta_k = \sigma_0/\sigma_k \end{array} \right\} \dots \dots \dots (c)$$

If the average stress of a specimen at time when the initial fracture takes place on the specimen, is shown by σ_{m1} or σ_{k1} by the above two expressions ((a), (b)) respectively, we can indicate one of the relations between fracture and rupture of a specimen by

$$\mu = \sigma_{k1}/\sigma_k \quad \text{or} \quad \sigma_{m1}/\sigma_m \dots \dots \dots (d)$$

The values of $\sigma_{m1}(\sigma_{k1})$, $\sigma_m(\sigma_k)$, $\beta_m(\beta_k)$ and μ obtained in all specimens are shown in Table 3, Figs. 10, 11 and 12 respectively, and the specimens ruptured are shown in Photos. 9~17. The results and the discussions are summarized as follows :

Table 3. Results of failure test of knotty specimens.

Specimen No.	$\sigma_{m1}(\sigma_{k1})$	$\sigma_m(\sigma_k)$	$\beta_m(\beta_k)$	μ	ϕ/b
	kg/cm ²	kg/cm ²			
1	660(760)	760(880)	1.64(1.42)	87	0.128
3	640(755)	920(1,085)	1.36(1.15)	70	0.150
5	510(625)	715(870)	1.74(1.43)	72	0.178
7	530(660)	650(810)	1.92(1.54)	81	0.195
9	510(625)	585(715)	2.13(1.75)	86	0.182
11	340(420*)	525(645*)	2.37(1.94*)	65	0.165
13	330(392*)	635(760*)	1.97(1.64*)	52	0.165
15	360(400*)	680(755*)	1.84(1.67*)	53	0.098
17	410(420*)	775(795*)	1.62(1.58*)	52	0.028

* Calculated under an assumption that tensile strength of sound knot itself is small enough to be neglected.

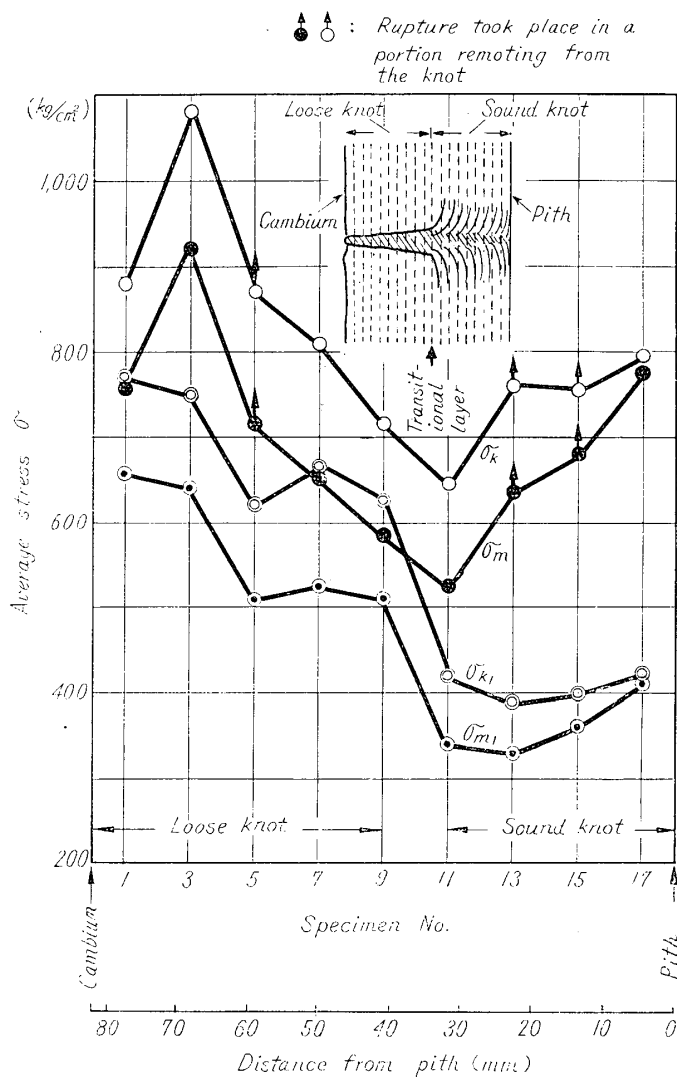


Fig. 10. Strength of knotty specimens as functions of distance from pith.

σ_k : Maximum stress calculated by reduced cross section of specimen.

σ_m : Maximum stress calculated by unreduced cross section of specimen.

σ_{k1} : Stress at first cracking calculated by reduced cross section of specimen.

σ_{m1} : Stress at first cracking calculated by unreduced cross section of specimen.

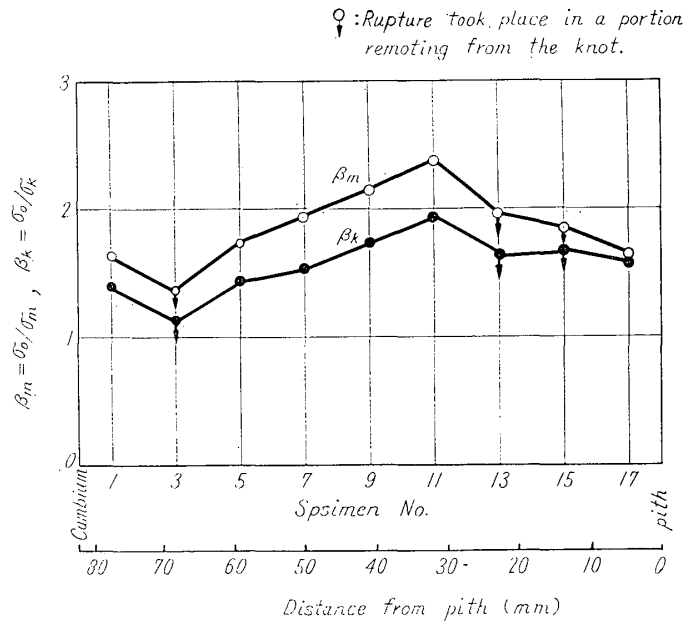


Fig. 11. β as functions of distance from pith.

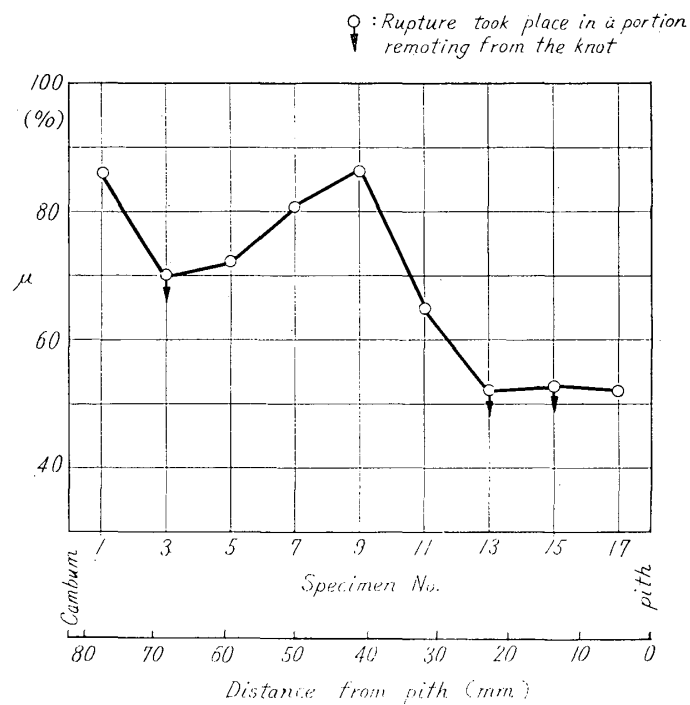


Fig. 12. β as functions of distance from pith.

i) As clearly shown in Fig. 10, the tensile strengths of these knotty plates varies in connection with the layers (specimen No.) or the types of the knots. The highest strength is found in a layer near the bark (specimen No. 3) and the lowest one in a transitional layer from sound knot to loose one (specimen No. 11).

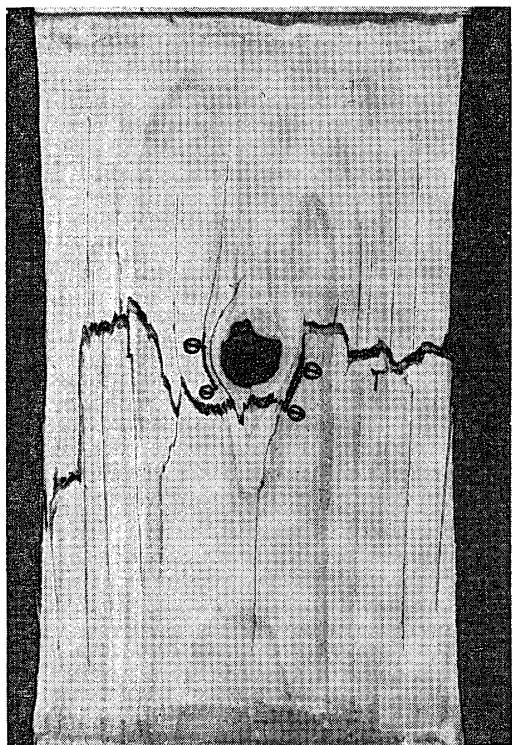


Photo. 9. Pith side face of knotty specimen after failure test (Specimen No. 1).

①-① : Fracture at $\sigma_{m1}=660 \text{ kg/cm}^2$
Maximum stress: $\sigma_m=760 \text{ kg/cm}^2$

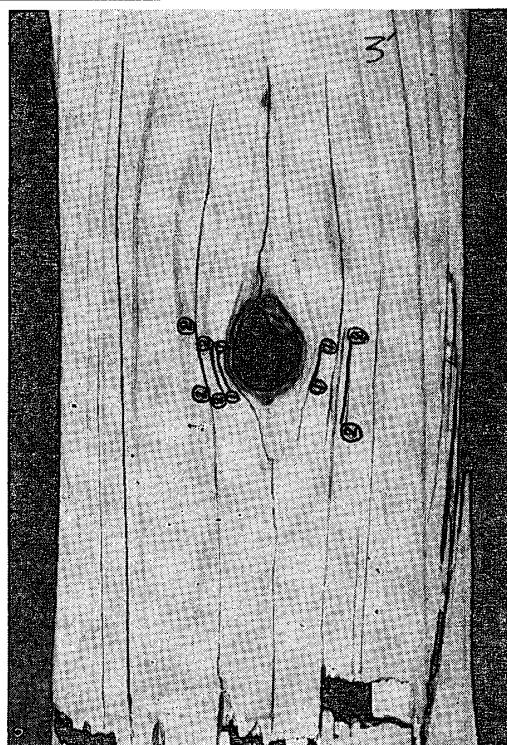


Photo. 10. Pith side face of knotty specimen after failure test (Specimen No. 3).

①-① : Fracture at $\sigma_{m1}=640 \text{ kg/cm}^2$
②-② : Fracture at $\sigma_{m2}=770 \text{ kg/cm}^2$
③-③ : Fracture at $\sigma_{m3}=890 \text{ kg/cm}^2$
Maximum stress: $\sigma_m=920 \text{ kg/cm}^2$

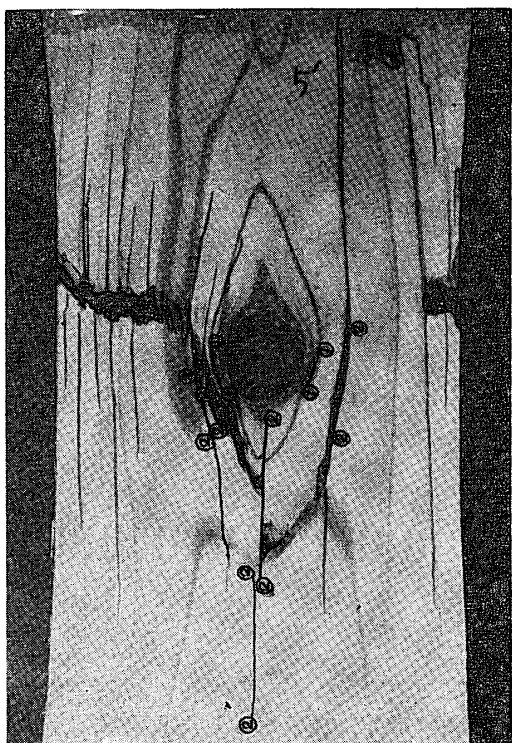


Photo. 11. Pith side face of knotty specimen after failure test (Specimen No. 5).

①-① : Fracture at $\sigma_{m1}=510 \text{ kg/cm}^2$
②-② : Fracture at $\sigma_{m2}=620 \text{ kg/cm}^2$
Maximum stress: $\sigma_m=715 \text{ kg/cm}^2$

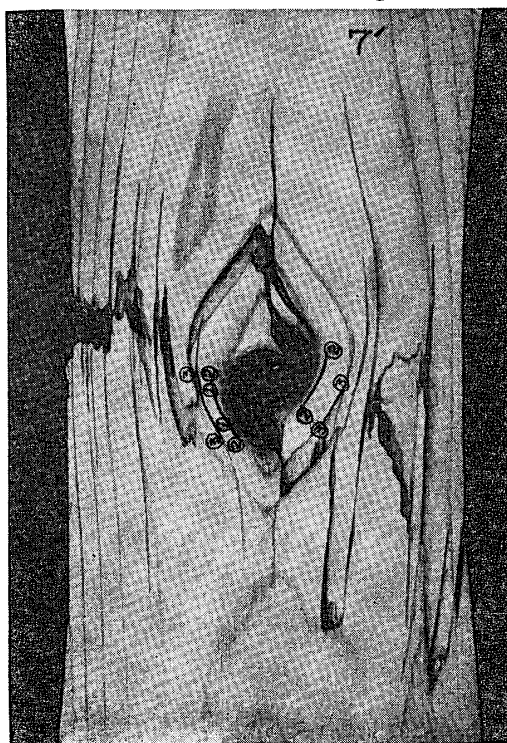


Photo. 12. Pith side face of knotty specimen after failure test (Specimen No. 7).

①-① : Fracture at $\sigma_{m1}=530 \text{ kg/cm}^2$
②-② : Fracture at $\sigma_{m2}=620 \text{ kg/cm}^2$
③-③ : Fracture at $\sigma_{m3}=640 \text{ kg/cm}^2$
Maximum stress: $\sigma_m=650 \text{ kg/cm}^2$

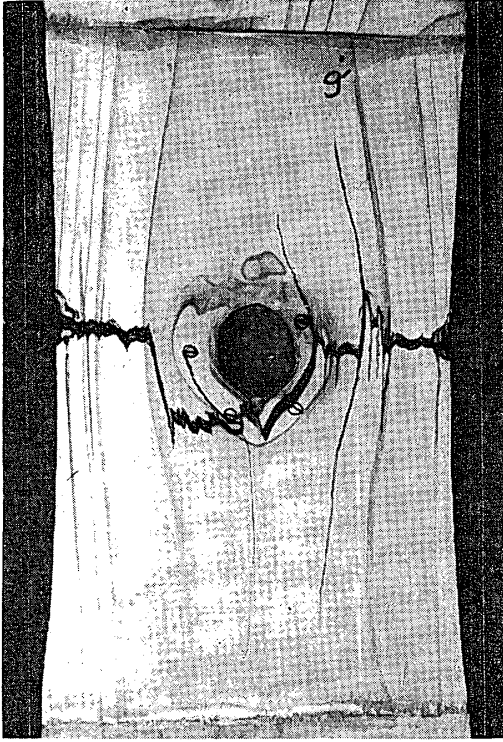


Photo. 13. Pith side face of knotty specimen after failure test (Specimen No. 9).
①-① : Fracture at $\sigma_{m1}=510 \text{ kg/cm}^2$
Maximum stress: $\sigma_m=585 \text{ kg/cm}^2$

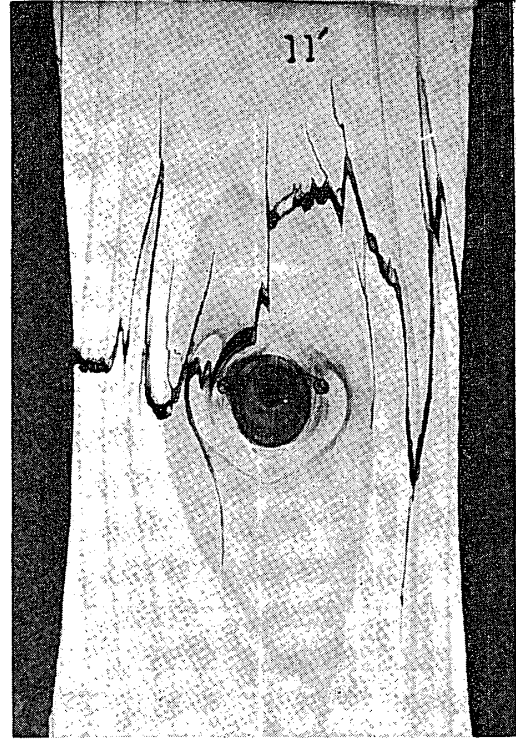


Photo. 14. Pith side face of knotty specimen after failure test (Specimen No. 11).
①-① : Fracture at $\sigma_{m1}=340 \text{ kg/cm}^2$
Maximum stress: $\sigma_m=525 \text{ kg/cm}^2$

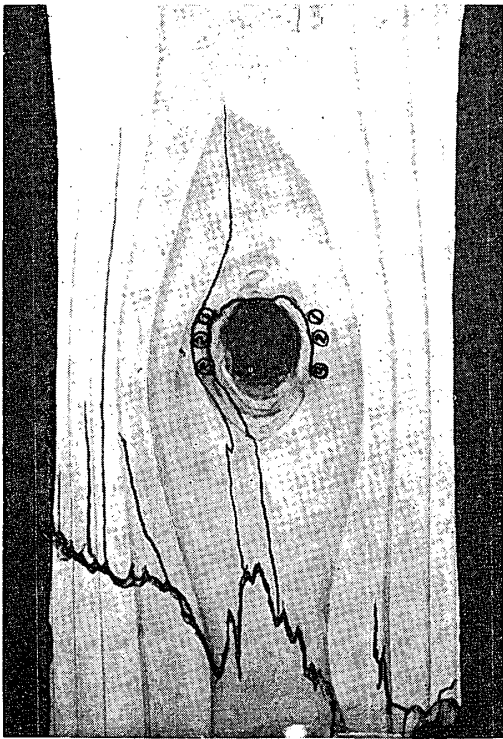


Photo. 15. Pith side face of knotty specimen after failure test (Specimen No. 13).
①-① : Fracture at $\sigma_{m1}=330 \text{ kg/cm}^2$
②-② : Fracture at $\sigma_{m2}=475 \text{ kg/cm}^2$
③-③ : Fracture at $\sigma_{m3}=580 \text{ kg/cm}^2$
Maximum stress: $\sigma_m=680 \text{ kg/cm}^2$

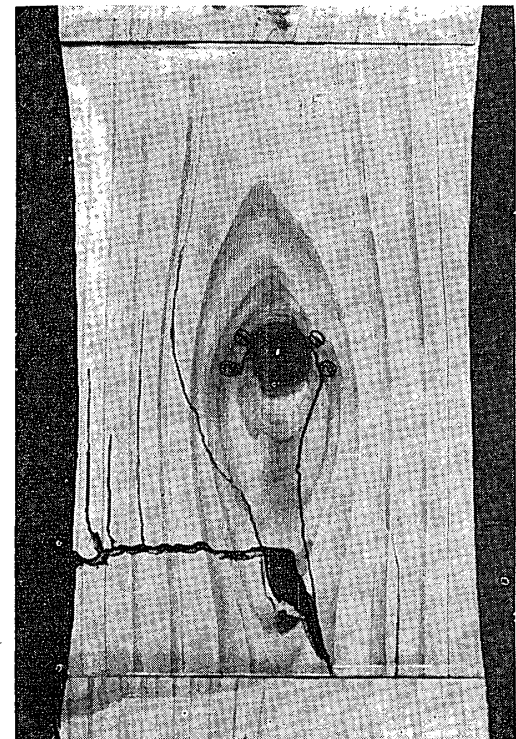


Photo. 16. Pith side face of knotty specimen after failure test (Specimen No. 15).
①-① : Fracture at $\sigma_{m1}=360 \text{ kg/cm}^2$
②-② : Fracture at $\sigma_{m2}=620 \text{ kg/cm}^2$
Maximum stress: $\sigma_m=680 \text{ kg/cm}^2$

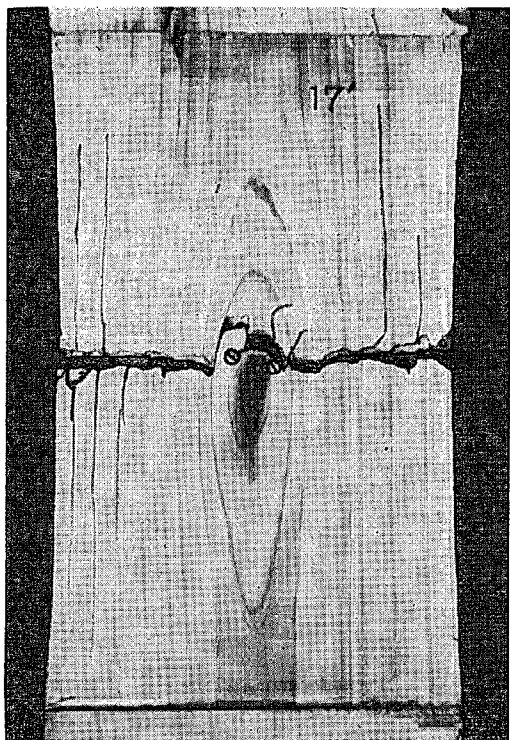


Photo. 17. Pith side face of knotty specimen after failure test (Specimen No. 17).

①-① : Fracture at $\sigma_{m1}=410 \text{ kg/cm}^2$
Maximum stress : $\sigma_m=775 \text{ kg/cm}^2$

tensile strength of a plate with a loose knot which is cut out of the layer remot-
ing fairly from the end of the sound knot, can be treated as an simply holed
plate.

iii) Fig. 12 shows that the value μ of sound knot plate is smaller than that
of loose knot plate. And the initial fractures of loose knot plates were localized
in the left or right lower portion of the knots as shown in Photos. 9~13, but those
of sound knot plates took place across the knot (Photos. 14 and 16) or around the
knot (Photos. 15 and 17).

iv) Rupture did not always pass through the local fractures (Photos. 10, 14,
15 and 16), in other words, shear stress in the surroundings of the knot seems
not to relate directly to the rupture.

v) In loose knot plates, rupture did not pass through the knot except No. 7
specimen (Photo. 12), even in which the rupture did not develop through the
maximum stress portions of the knot border but a slip took place at the upper
and lower side of the border. From these facts and the distribution of strain
shown before, it is concluded that the border of a loose knot has higher elasticity
and higher strength than the other portions, namely, it is said that the loose knot
is reinforced by the border

It can be considered that the more the
layer remotes from the transitional layer,
the higher the strength of the knotty
plate is. These reasons seem to be that the
sound knot disturves the grain of the sur-
roundings more than the loose knot does.

ii) In Fig. 11, both β_m and β_k are larger
than 1. Their maximum value of $\beta_k=1.94$
and $\beta_m=2.37$ are found in the transitional
layer (specimen No. 11), and the minimum
values are $\beta_k=1.15$ and $\beta_m=1.36$ of the
specimen No. 3.

H. WINTER⁸⁾ defined experimentally the
“Kerbfactor” a_k of the artificially holed
wood plates (where, a_k is equal to the re-
ciprocal of β_k), and from his results, it is
said that a_k is influenced by the value ϕ/b
(ϕ : diameter of knot, b : width of specimen),
but in the range of ϕ/b as in the present
paper, a_k is generally about $0.8\sim0.9$ or β_k
 $=1.1\sim1.2$. We know, therefore, that the

T. MORI³⁾ carried out many experiments on the tensile strength of knotty wood, and reported that the tensile strength of knotty wood can be calculated approximately by the following formula :

$$\sigma_m = \sigma_0(1 - \phi/b) \dots\dots\dots(1)$$

σ_0 : tensile strength of knot-free specimen

ϕ : diameter of knot

b : width of specimen

This formula means nothing but that the strength of every knot itself can be considered as zero, and that of the surroundings of a knot can be considered to equal to that of knot-free plates.

The application of formula (1) was tried on the results obtained in the present paper. But, as shown in Fig. 13, the experimental results remote far from formula (1) and, therefore, the application is hopeless on such a thin plate, and it will be suggested that formula (1) must be applied within some range of thickness of materials.

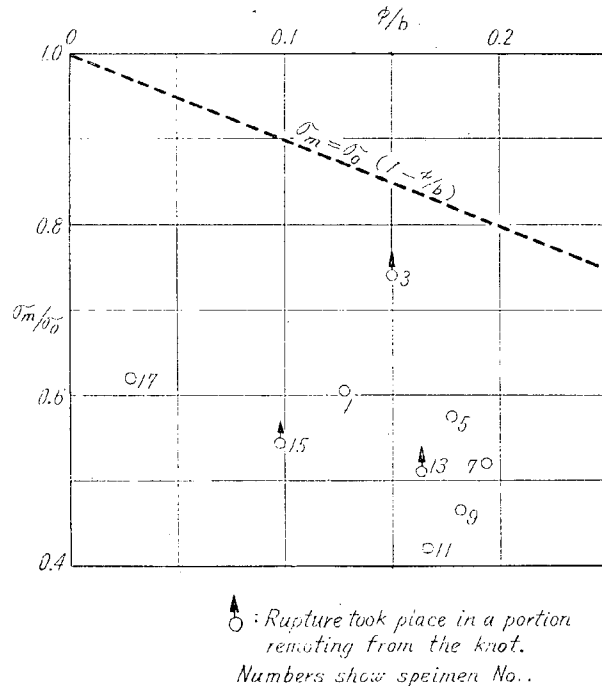


Fig. 13. Relation between σ_m/σ_0 and ϕ/b of knotty specimen in comparison with eq. (1).

Summary

Tensile load was applied to the knotty plates shown in Fig. 1 and the strain distribution was determined by means of brittle coating method, and the fracture and the rupture were observed. The results and discussion are summarized as follows :

1) Strain distribution

The crack pattern of coating (Photos. 2~7) differs considerably from that of a simply holed plate (Photo. 8). Distribution of principal strains around a knot are very irregular (Figs. 3~8, Photos. 2~7) and there is some large shear strain along fiber (Fig. 9). The maximum value of the tensile strain does not always appear around a knot (Figs. 5, 6, 8), and the strain concentration near a knot is not higher than double of the average strain (Figs. 3~8).

2) Fracture and rupture

The tensile strength of the transitional layer from sound knot to loose knot, is the lowest (Fig. 10) and that of the layer near bark is the highest and similar to

that of simply holed plates. The loose knot can be considered to be reinforced by the border. MORI's experimental formula (1) was examined and it was concluded that the formula could not be applied to such a thin plate (Fig. 13).

Literature Cited

- 1) GRAF, O. : Masch.-Bau 8 : 642 (1929)-KOLLMANN, F. : Techn. d. Holzes u. H., 1 : 662, Berlin (1951)
- 2) GABER, E. : Bautechn. 14 : 64 (1935)
- 3) MORI, T. : KENCHIKU GAKKAI RONBUNSHŪ (Transaction of the Institute of Japanese Architects) 8 : 1 (1938) (in Japanese, Engl. summary)
- 4) YLINEN, A. : Holz als Roh- u. W. 5 : 337 (1942)
- 5) MAKU, T. and H. SASAKI : MOKUZAI GAKKAISHI (Jour. Japan Wood Res. Soc.) 6 : 58, 63, 67, 214 (1960) (in Japanese, Engl. summary)
- 6) SASAKI, H. : ZAIRYŌ SHIKEN (Jour. Japan Soc. Test. Mat.) 10 : 887 (1961) (in Japanese)
- 7) MOKUZAI KŌGYŌ (Wood Industry) 9-12 (1954-1957)
- 8) WINTER, H. : Richtlinien für den Holzflugzeugbau F. IIIa, Berlin (1944)-KOLLMANN, F. : Techn. d. Holzes u. H. 1 : 672, Berlin (1951)

摘 要

Fig. 1 および Table 1 にしめすような、中央部にそれぞれ節をもった、一連のヒノキ挽板について、両端に引張力をあたえた場合のひずみの分布状態と局所的な破壊の進行および破断力を測定した。ここで用いたひずみの測定方法はこれまでに報告した⁵⁾⁶⁾ぜい性塗膜法である。実験結果とその考察を要約すると以下ようになる：

—まず、ひずみの分布状態について—

1. 有節板の表面にほどこしたぜい性塗膜のき裂模様 (Photos. 2~7) は人為的に作った有孔板のそれ (Photo. 8) と著しく相違する。
2. 死(抜)節のひずみ分布は節の上下方向に対称的ではない (Photos. 2~5)。
3. 生節では節の上下に2次元の等価な引張ひずみが分布する領域が現われる (Photos. 6, 7)。
4. 節の近くの引張主ひずみの方向は、とくに死節では著しく乱れており (Photos. 2~5, Figs. 3~6), このあたりでは繊維にそう大きなせん断応力が生じている (Fig. 9)。
5. 引張主ひずみの最大値は必ずしも節の近くに生ずるとは限らず、木理の状態によつては試験片の端部に生ずることもある (Figs. 5, 6, 8)。
6. 節の近くは節の周縁部あるいは節自身より一般に大きな変形をしているが、その最大値は平均ひずみのせいぜい2倍程度でしかない (Figs. 3~8)。

—破壊(断)テストの結果について—

試片の幅を b 厚さを h , 節の直径を ϕ , 最初の破壊が生じたときの荷重を P_1 , 破断したときの荷重を P , 無節材の強さを σ_0 とし,

$$\begin{aligned}\sigma_m &= P/bh, & \sigma_k &= P/(b-\phi)h, \\ \sigma_{m1} &= P_1/bh, & \sigma_{k1} &= P_1/(b-\phi)h,\end{aligned}$$

$$\beta_m = \sigma_0 / \phi_m, \quad \beta_k = \sigma_0 / \sigma_k, \\ \mu = \sigma_{k1} / \sigma_k = \sigma_{m1} / \sigma_m$$

で表わすと

1. 有節材の強さ (σ_m, σ_k) は樹皮の近くでもつとも高く、生節から死節へ移行する層でもつとも低くなる (Fig. 10)。
 2. β の値は β_m, β_k のいずれについても 1 より大きく、その値は樹皮の近くの層では人為的に円孔をあけた場合⁸⁾と変らないが、他の層では著しく大きい (Fig. 11)。
 3. 生節の μ の値は死節のそれに較べるとはるかに小さく、生節が周辺部の木理を乱す程度は死節とくに生節から十分離れたそれに較べると著しいと考えられる (Fig. 12)。
 4. 破断の状態からみて、局所的な破壊が試片の破断に関係していると考えられる場合 (Photos. 8, 10, 11, 12, 17) と無関係に思われる場合 (Photos. 9, 13, 14, 15) がみられる。
 5. 死節の周縁部は一種の補強の役割をなしているようで、この部分の弾性係数と強さは共に大きいと考えられ、この部分が破壊されることはまれである (Photos. 2~5, Figs. 3~6)。
 6. 森³⁾の有節材の破壊に関する“直径比説”(式(1))が本実験のような薄板にも適用できるかどうかを検討した結果は否定的で、式(1)は厚さの制限を必要とするものと考えられる。
- 最後に本実験に大いに協力して頂いた勝山三千代夫人と佐々木正明君に感謝の意を表する。